

Antiferromagnetic cavity optomagnonics

T. S. Parvini* and V. A. S. V. Bittencourt†

Max Planck Institute for the Science of Light, Staudtstr. 2, PLZ 91058, Erlangen, Germany

Silvia Viola Kusminskiy‡

Max Planck Institute for the Science of Light, Staudtstr. 2, PLZ 91058, Erlangen, Germany and Institute for Theoretical Physics, University Erlangen-Nürnberg, Staudtstr. 7, 91058 Erlangen, Germany

We propose a cavity optomagnetic system based on antiferromagnetic insulators. We derive the Hamiltonian of the system and obtain the coupling of the antiferromagnetic magnon modes to the optical cavity field as a function of magnetic field and material properties. We show that, in the presence of hard-axis anisotropy, the optomagnetic coupling can be tuned by a magnetic field applied along the easy axis, allowing to bring a selected magnon mode into and out of a dark mode. For easy-axis antiferromagnets the coupling is instead independent of the magnetic field. We study the dynamic features of the driven system including optically induced magnon amplification and cooling, Purcell enhancement of transmission, and induced transparency, and discuss their experimental feasibility.

Introduction.— The interaction between light and magnetism at the quantum level holds promise for future data storage and processing technologies. In seminal recent experiments, the coherent coupling of magnons (the spin-wave quanta) to optical photons has been demonstrated in solid state optomagnetic cavities [1–3]. The latter are dielectric magnetic structures capable of simultaneously confining light and magnons, providing an enhancement of the magnon-photon coupling and enabling the study of cavity effects in a new platform. Magnons in these structures exhibit good coherence properties and tunable frequencies, and can couple strongly to microwave (MW) cavity fields [4–10]. Quantum memories [11–17] or transducers are possible applications [18, 19].

Optomagnetic cavities have been investigated so far within the scope of ferromagnetic (FM) magnons. Experimentally, Yttrium Iron Garnet (YIG) cavities are used, supporting magnons with frequencies of the order of GHz (note that although YIG is technically a *ferrimagnet*, one sublattice has a much larger spin and is dominant) [1–3, 20–22]. Theoretically, several phenomena have been studied, including transmission properties [23], nonlinear dynamics [24] and magnetic textures [25], and magnon cooling [26] and heralding [27].

Antiferromagnetic (AFM) materials support magnons that can be described as excitations of a spin anti-aligned ground state (the Néel state) [28]. The AFM dynamics is typically in the THz range, which could enable ultrafast information processing and communication [29–32]. At the same time, AFMs are robust against magnetic perturbations, an attractive feature for data storage [33, 34]. Strong coupling between MW photons and AFM magnons in an organic compound [35] has been reported, while theoretical studies have shown the possibility of re-

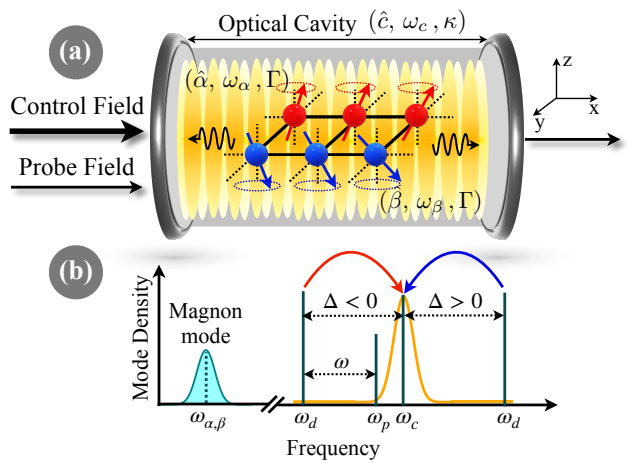


Figure 1. (a) Schematic illustration of the antiferromagnetic optomagnetic cavity. The homogeneous magnon modes $\hat{\alpha}$ and $\hat{\beta}$ with frequencies $\omega_{\alpha,\beta}$ and decay rates $\Gamma_{\alpha,\beta}$ couple to a cavity mode \hat{c} with frequency ω_c and decay rate κ . (b) Pump scheme: Ω_m , ω_c , ω_d , ω_p , magnon, optical cavity resonance, drive, and probe frequencies respectively. The detuning of the drive is $\Delta = \omega_d - \omega_c$, and $\omega = \omega_p - \omega_d$.

alizing a magnon dark mode [36] and coupling to ferromagnets [37] via a microwave cavity. In turn, methods involving light to probe and control AFMs are being developed [38]. Nevertheless, AFMs are still unexplored as platforms for optomagnetic cavities.

In this letter, we propose a novel solid state cavity optomagnetic system based on an antiferromagnetic insulator. We study the interaction of the AFM magnon modes with light confined in the AFM material. We derive the Hamiltonian governing the system and show that in the presence of hard-axis anisotropy the optomagnetic coupling to both homogeneous magnon modes can be tuned by an external magnetic field. In particular, we show that the magnon modes can be selectively

* tahereh.parvini@mpl.mpg.de

† victor.bittencourt@mpl.mpg.de

‡ silvia.viola-kusminskiy@mpl.mpg.de

decoupled from the cavity, rendering them dark. With the obtained Hamiltonian, we characterize the dynamical response of the system and discuss the experimental feasibility of our proposal.

Model.— We consider an AFM insulator consisting of two magnetic sublattices A and B of opposite spin. The AFM hosts two homogeneous magnon modes $\hat{\alpha}$ and $\hat{\beta}$, see Fig. 1, and is at the same time an optical cavity, in analogy to dielectric optomechanical resonators [39] and to optomagnetic cavities made of YIG [1–3]. AFMs with a high index of refraction and low absorption in the optical range, such as NiO ($n \approx 2.4$) [40] would serve the purpose, or heterostructures containing MnF₂ ($n \approx 1.4$) [41] or FeF₂ ($n \approx 1.5$) [42]. The Hamiltonian of the coupled system is

$$\hat{\mathcal{H}} = \hat{\mathcal{H}}_{\text{ph}} + \hat{\mathcal{H}}_{\text{AFM}} + \hat{\mathcal{H}}_{\text{OM}}, \quad (1)$$

with $\hat{\mathcal{H}}_{\text{ph}}$ and $\hat{\mathcal{H}}_{\text{AFM}}$ the free photonic and antiferromagnetic Hamiltonians, respectively. $\hat{\mathcal{H}}_{\text{OM}}$ contains the coupling between the AFM magnons and the cavity photons, and is our main result in this section.

The quantized optical field in the cavity is $\hat{\mathbf{E}}(\mathbf{r}, t) = 1/2 \sum_{\xi} \left(\mathbf{E}_{\xi}(\mathbf{r}) \hat{c}_{\xi}(t) + \mathbf{E}_{\xi}^*(\mathbf{r}) \hat{c}_{\xi}^\dagger(t) \right)$ with $\hat{c}_{\xi}^{(\dagger)}$ annihilation (creation) operator of mode ξ with resonance frequency ω_{ξ} , and hence $\hat{\mathcal{H}}_{\text{ph}} = \hbar \sum_{\xi} \omega_{\xi} \hat{c}_{\xi}^\dagger \hat{c}_{\xi}$. The antiferromagnetic Hamiltonian, $\hat{\mathcal{H}}_{\text{AFM}}$, consists of (i) the exchange interaction between nearest-neighbor spins $J \sum_{\langle i \neq j \rangle} \hat{\mathbf{S}}_i \cdot \hat{\mathbf{S}}_j$ ($J > 0$), (ii) the Zeeman interaction between spins and an external DC magnetic field \mathbf{B}_0 along \mathbf{e}_z , $|\gamma| B_0 \sum_i \hat{\mathbf{S}}_i^z$ (γ gyromagnetic ratio), and (iii) easy $-\frac{K_{\parallel}}{2} \sum_i (S_i^z)^2$ ($K_{\parallel} > 0$) and hard $\frac{K_{\perp}}{2} \sum_i (S_i^x)^2$ ($K_{\perp} \geq 0$) axis anisotropy in the \mathbf{e}_z and \mathbf{e}_x directions respectively. For small magnetization fluctuations around the Néel ordered state, the Holstein-Primakoff (HP) transformations [43, 44] can be used to express $\hat{\mathcal{H}}_{\text{AFM}}$ in terms of bosonic operators $\hat{a}_{\mathbf{k}}$ and $\hat{b}_{\mathbf{k}}$ associated with the sublattices A and B . To first order, the HP transformations are given in terms of spin ladder operators as $\hat{S}_{A(B)}^+ = \sqrt{2S/N} \sum_{\mathbf{k}} e^{-i\mathbf{k} \cdot \mathbf{x}_i} \hat{a}_{\mathbf{k}} (\hat{b}_{\mathbf{k}}^\dagger)$, where N is the total number of sites per sublattice and S the spin on each site. $\hat{\mathcal{H}}_{\text{AFM}}$ is diagonalized via a 4D Bogoliubov transformation to the bosonic operators $\hat{\alpha}_{\mathbf{k}} = u_{\alpha,a} \hat{a}_{\mathbf{k}} + v_{\alpha,b} \hat{b}_{-\mathbf{k}}^\dagger + v_{\alpha,a} \hat{a}_{-\mathbf{k}}^\dagger + u_{\alpha,b} \hat{b}_{\mathbf{k}}$ and $\hat{\beta}_{\mathbf{k}} = u_{\beta,a} \hat{a}_{\mathbf{k}} + v_{\beta,b} \hat{b}_{-\mathbf{k}}^\dagger + v_{\beta,a} \hat{a}_{-\mathbf{k}}^\dagger + u_{\beta,b} \hat{b}_{\mathbf{k}}$ (see Sup. Mat. [45] for details). In this representation $\hat{\mathcal{H}}_{\text{AFM}} = \hbar \sum_{\mathbf{k}} [\omega_{\alpha\mathbf{k}} \hat{\alpha}_{\mathbf{k}}^\dagger \hat{\alpha}_{\mathbf{k}} + \omega_{\beta\mathbf{k}} \hat{\beta}_{\mathbf{k}}^\dagger \hat{\beta}_{\mathbf{k}}]$ with $\omega_{\alpha,\beta\mathbf{k}}$ the respective eigenfrequencies. In this work we restrict our analysis to the two homogeneous ($\mathbf{k} = 0$) AFM magnon modes, hence from now onwards we drop the dependence on \mathbf{k} . The corresponding magnon frequencies $\omega_{\alpha,\beta}$ are functions of the characteristic frequencies $\omega_E = \hbar J S N$, $\omega_{\parallel,\perp} = \hbar S N K_{\parallel,\perp}$, and $\omega_H = |\gamma| B_0$: $\omega_{\alpha(\beta)}^2 = \omega_H^2 + \omega_E \omega_{\perp} + 2\omega_E \omega_{\parallel} + \omega_{\perp} \omega_{\parallel} + \omega_{\parallel}^2 \pm$

$\sqrt{\omega_E^2 \omega_{\perp}^2 + 4\omega_E \omega_H^2 (\omega_{\perp} + 2\omega_{\parallel}) + \omega_H^2 (\omega_{\perp} + 2\omega_{\parallel})^2}$ [37, 46, 47]. In our notation, $\omega_{\alpha} \geq \omega_{\beta}$ and therefore α (β) labels the upper (lower) mode [47]. Whereas ω_{α} increases with the magnetic field, ω_{β} decreases and goes to zero at the onset of the spin-flop phase at $\omega_{SF} \approx \sqrt{2\omega_E \omega_{\parallel}}$ [48].

The interaction between light and magnetization is described by the magneto-optical coupling [49, 50] $\mathcal{H}_{\text{MO}} = \sum_{i,\mu,\nu} E_{\mu}^*(\mathbf{r}_i) \varepsilon_{\mu\nu}(S_i) E_{\nu}(\mathbf{r}_i)$, where $i \in A, B$ indicates the lattice site and $\varepsilon_{\mu\nu}$ ($\mu, \nu = x, y, z$) is the spin-dependent part of the permittivity tensor. In this letter we consider simple cubic and rutile-structure AFMs, other more complex structures will be considered elsewhere. For these materials, within linear response in the deviations from the magnetic equilibrium, \mathcal{H}_{MO} reduces to [45, 49, 50]

$$\begin{aligned} \mathcal{H}_{\text{MO}} = & K_+ \sum_{i \in A, j \in B} \left[P_i^+ (S_-^i + S_-^j) - P_i^- (S_+^i + S_+^j) \right] \\ & + K_- \sum_{i \in A, j \in B} \left[P_i^+ (S_+^i - S_+^j) - P_i^- (S_-^i - S_-^j) \right], \end{aligned} \quad (2)$$

where $P_i^{\pm} = E_z^*(\mathbf{r}_i) E_{\pm}(\mathbf{r}_i) - E_{\pm}^*(\mathbf{r}_i) E_z(\mathbf{r}_i)$, with $E_{\pm} = E_x \pm iE_y$ and $S_{\pm} = S_x \pm iS_y$. We have assumed that the electric field varies smoothly, such that $P_i^{\pm} \approx P_j^{\pm}$ for nearest neighbors. The linear magneto-optic coefficients K_{\pm} correspond to processes in which the two sublattices scatter the light in-phase (+) or out-of-phase (-). For our purposes, one-magnon scattering processes coming from quadratic terms in the spin (e.g. $\propto \hat{S}^z \hat{S}^{\pm}$) can be absorbed in the definition of K_{\pm} . This model applies e.g. to the uniaxial AFMs MnF₂ or FeF₂ [51, 52], and for the simple cubic AFM NiO for which $K_- = 0$.

We obtain the optomagnetic coupling Hamiltonian $\hat{\mathcal{H}}_{\text{OM}}$ by quantizing Eq. (2). We focus on the interaction between the homogeneous AFM magnon modes $\hat{\alpha}$ and $\hat{\beta}$ with a *single* optical mode \hat{c} with frequency ω_c , analogous to the scenario often considered in cavity optomechanics [39]. For an optical mode with circular polarization in the yz plane, from Eq. (2) we obtain [45]

$$\hat{\mathcal{H}}_{\text{OM}} = -\hbar G \hat{c}^\dagger \hat{c} (g_{\alpha} \hat{\alpha}^\dagger + g_{\beta} \hat{\beta}^\dagger + \text{h.c.}), \quad (3)$$

with (ε is the AFM dielectric constant)

$$G = \frac{\omega_c K_+}{4\varepsilon} \sqrt{2SN}. \quad (4)$$

The AFM optomagnetic coupling depends on the Bogoliubov coefficients through

$$g_{\alpha(\beta)} = (u_{\alpha(\beta)}^+ + v_{\alpha(\beta)}^+) + K (u_{\alpha(\beta)}^- + v_{\alpha(\beta)}^-) \quad (5)$$

where $K = K_-/K_+$ quantifies the intrinsic magneto-optical asymmetry between the sublattices, and we have defined $u_{\alpha(\beta)}^{\pm} = u_{a,\alpha(\beta)} \pm u_{b,\alpha(\beta)}$ and $v_{\alpha(\beta)}^{\pm} = v_{a,\alpha(\beta)} \pm v_{b,\alpha(\beta)}$. Hence, the two AFM magnon modes $\hat{\alpha}$ and $\hat{\beta}$

couple, in general, with different strength to the cavity mode.

Optomagnetic Coupling.— The constant G describes the coupling to the magnetization's fluctuations sector and is consistent with the one derived in Ref. [24] for the optomagnetic coupling in a ferromagnetically ordered system. Assuming equivalent sublattices with Faraday rotation per unit length θ_F , $G = \left(1/\sqrt{2NS}\right) (c\theta_F/4\sqrt{\varepsilon})$ (c speed of light). The $1/\sqrt{N}$ dependence indicates that the density of excitations is relevant for the coupling, favoring small magnetic volumes. Due to the lack of data on absolute values for K_+ (or θ_F) for simple AFMs, we take as an estimate for G the value for $(1\mu\text{m})^3$ YIG (diffraction limit volume), $G_{\text{YIG}} = 0.1\text{MHz}$ [24]. Some measurements indicate that the Faraday rotation coefficient in AFMs can be quite large, e.g. similar values as for YIG have been reported for BiFeO₃ [53]. Note that G given in Eq. (21) assumes perfect mode matching. Imperfect mode overlap can be accounted for by a mode-volume ratio factor [24] and it is responsible for a suppression of the coupling in current experiments with YIG [18, 54]. The second term in Eq. (5) gives a contribution proportional to KG and describes the coupling to fluctuations of the Néel vector. Typical values of K are $K \approx 0.01$ (e.g. for MnF₂ or FeF₂ [51]).

The reduced couplings $g_{\alpha,\beta}$ can be found analytically, but the general solution is lengthy and we will not give it here. Simple expressions can be given in certain cases. Since the exchange energy is usually the largest energy scale in the AFM, the condition $\omega_{\perp,\parallel} \ll \omega_E$ holds. For an easy-axis AFM ($\omega_\perp = 0$), we obtain [45]

$$g_{\alpha,\beta}^{\omega_\perp=0} \approx \left(\frac{\omega_\parallel}{2\omega_E}\right)^{1/4} \pm K \left(\frac{2\omega_E}{\omega_\parallel}\right)^{1/4}. \quad (6)$$

Note that Eq. (6) is independent of the magnetic field \mathbf{B}_0 , a consequence of the axial symmetry of the system in this case [45]. In the absence of magneto-optical asymmetry ($K = 0$) both modes couple equally to the light field, while for finite K , $g_\alpha^{\omega_\perp=0}$ increases linearly and $g_\beta^{\omega_\perp=0}$ decreases. If the condition $K = \sqrt{\omega_\parallel/2\omega_E}$ is met, then $g_\beta^{\omega_\perp=0} = 0$ and the β mode is a dark mode, completely decoupled from the cavity mode. Whereas this requires fine tuning, it could be achievable in cold atoms realizations where the relevant parameters can be tuned [55–59]. The situation nevertheless changes in the presence of hard-axis anisotropy, where the coupling to the modes can be tuned externally by the magnetic field as we show below. From Eq. (6) we obtain $g_{\alpha,\beta}^{\text{MnF}_2} \approx 0.5, 0.4$ ($\omega_E = 9.3\text{ THz}$, $\omega_\parallel = 0.15\text{ THz}$, $K = 0.007$ [51, 60]) and $g_{\alpha,\beta}^{\text{FeF}_2} \approx 0.6, 0.7$ ($\omega_E = 9.5\text{ THz}$, $\omega_\parallel = 3.5\text{ THz}$, $K = 0.01$ [49, 61]).

In the absence of a magnetic field, $\hat{\mathcal{H}}_{\text{AFM}}$ is invariant under the transformation $\hat{a}_k \longleftrightarrow \hat{b}_{-k}$. For finite hard-axis anisotropy ($\omega_\perp \neq 0$), imposing this symmetry we

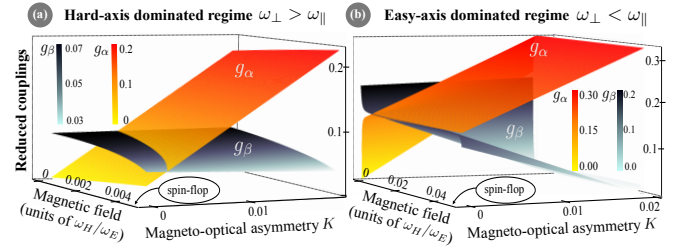


Figure 2. Reduced optomagnetic coupling coefficients g_α and g_β , as a function of external bias magnetic field (as ω_H/ω_E) and of the magneto-optical asymmetry K . Parameters: (a) $\omega_\parallel/\omega_E = 1.3 \times 10^{-5}$, $\omega_\perp/\omega_E = 7.6 \times 10^{-4}$ (NiO); (b) $\omega_\perp/\omega_E = 1.3 \times 10^{-5}$, $\omega_\parallel/\omega_E = 7.6 \times 10^{-4}$.

obtain [45]

$$\begin{aligned} g_\alpha^{\omega_H=0, \omega_\perp \neq 0} &= 2K(u_{\alpha,a} - v_{\alpha,a}), \\ g_\beta^{\omega_H=0, \omega_\perp \neq 0} &= 2(u_{\beta,b} - v_{\beta,b}), \end{aligned}$$

which implies that for $K = 0$ $\hat{\alpha}$ is a dark mode ($g_\alpha = 0$) whereas the β -mode is independent of K . The case $\omega_\perp = \mathbf{B}_0 = 0$ is however pathological, since $\hat{\alpha}$ and $\hat{\beta}$ are degenerate. Then Eq. (6) holds, with $g_\alpha = g_\beta \neq 0$ (the Bogoliubov coefficients present a discontinuity at $\omega_\perp = 0$).

Fig. 2 shows $|g_\alpha|$ and $|g_\beta|$ as a function of the external magnetic field and of K for representative finite anisotropy values ω_\perp and ω_\parallel . In Fig. 2 (a) we took these as for NiO ($\omega_\parallel/\omega_E = 1.3 \times 10^{-5}$ and $\omega_\perp/\omega_E = 7.6 \times 10^{-4}$ [62]), and in Fig. 2 (b) we inverted these such that $\omega_\parallel > \omega_\perp$. We see that in both cases the coupling strengths $g_{\alpha,\beta}$ can be tuned by \mathbf{B}_0 , although with some qualitative differences. For $K = 0$ the α -mode can be tuned from dark to bright by increasing \mathbf{B}_0 , with a slow linear increase for $\omega_\parallel < \omega_\perp$ and rapidly but saturating for $\omega_\parallel > \omega_\perp$. For both cases there is a threshold K_{th} such that for $K > K_{\text{th}}$, there exists a finite \mathbf{B}_0 for which the β -mode is rendered dark ($g_\beta = 0$). In the regime considered for Fig. 2, $g_{\alpha,\beta} < 1$ for all fields, since the maximum \mathbf{B}_0 is limited by the spin-flop transition. This suppresses the corresponding optomagnetic coupling ($Gg_{\alpha,\beta}$). g_α increases nevertheless rapidly with K , so materials with a larger magneto-optical asymmetry would be favorable for larger coupling values. Our calculations indicate that $K \gtrsim 0.1$ would be sufficient for $g_\alpha > 1$ [45].

A figure of merit for determining the strength of the coupling is the cooperativity [39]. Taking $G = 0.1\text{MHz}$ as noted above, and typical values for the magnon ($\Gamma \approx 1\text{GHz}$ [63, 64]) and optical cavity decay rates ($\kappa \approx 100\text{MHz}$ [1]), for $g_{\alpha,\beta} = 1$ we obtain a single-photon cooperativity $\mathcal{C}_{\alpha,\beta}^0 = 4G^2 g_{\alpha,\beta}^2 / \Gamma \kappa \approx 4 \times 10^{-6}$. For an estimated maximum photon density of $10^5/\mu\text{m}^3$ allowed in the cavity [24], the cooperativity $\mathcal{C}_{\alpha,\beta} = n_c \mathcal{C}_{\alpha,\beta}^0$ (with $n_c = \langle \hat{c}^\dagger \hat{c} \rangle$ steady state number of photons circulating in the cavity) could be therefore tuned into the strong coupling regime ($\mathcal{C}_{\alpha,\beta} > 1$) by reaching $g_{\alpha,\beta} > 1$. Improved

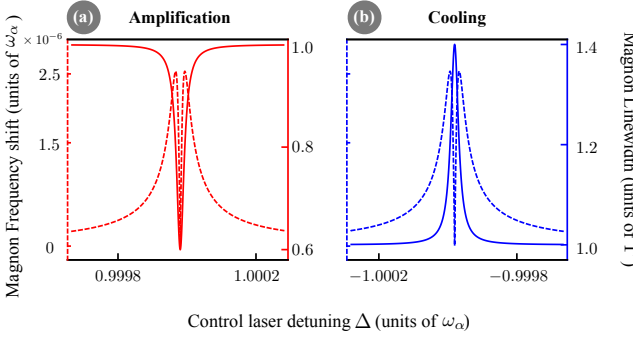


Figure 3. Effective linewidth (solid line) and frequency shift (dotted line) of the magnon α -mode vs. detuning Δ/ω_α for (a) blue-detuned and (b) red-detuned control light. Parameters: $\omega_\alpha/\omega_E = 4 \times 10^{-2}$ (NiO), $\Gamma/\omega_E = \kappa/\omega_E = 10^{-6}$ and $g_\alpha G\sqrt{n_c}/\omega_E = \sqrt{10^5} 10^{-9}$.

cavity and magnon decay rates would boost this value further. In this regime, magnons and photons hybridize and coherent exchange of information is possible.

Dynamical Response.— We now consider that the cavity is driven by a strong control laser with amplitude s_d and frequency ω_d , and a weak probe laser with amplitude s_p and frequency ω_p , see Fig. 1. Correspondingly, we add a driving term $\hat{\mathcal{H}}_D = i\hbar\sqrt{\eta\kappa}(\hat{c}_\xi^\dagger s_{in} + H.c.)$ to the Hamiltonian in Eq. (1), where $s_{in} = s_d e^{-i\omega_d t} + s_p e^{-i\omega_p t}$. The total loss rate of the optical cavity is $\kappa = \kappa_{ex} + \kappa_0$, where κ_{ex} and κ_0 correspond to the loss rates due to external coupling and intrinsic dissipation, respectively. The coupling efficiency $\eta = \kappa_{ext}/\kappa_0$ is adjustable in experiments [65, 66].

In the following we restrict our results to the resolved sideband regime, $\omega_{\alpha,\beta} \gg \kappa$. Since the magnon frequencies for AFMs are in the THz range, this condition is not very restrictive. The optomagnonic coupling Eq. (3) leads to the modification of both the magnon resonance frequency (optical spring effect) and the magnon damping (optomagnonic damping). Fig. 3 shows an example of these for the α -mode as a function of detuning of the control laser for $C_\alpha = 0.4$. The resulting frequency shift corresponds to MHz. For blue detuning, Stokes processes are driven and the effective magnon linewidth decreases near the resonance, indicating amplification. For stronger coupling this can lead to instabilities and the breakdown of the linearized model [23, 24]. In the red-detuned regime the linewidth increases when approaching resonance, indicating the conversion of magnons to photons via anti-Stokes processes. This regime can be used to cool the magnon mode if the decay rate of photons is faster than the magnon decay rate [26]. The β -mode presents qualitatively analogous behavior. These effects depend on the external magnetic field *via* the couplings $g_{\alpha,\beta}$, see Fig. 2.

Finally, we turn our attention to the transmission and reflection properties of the AFM optomagnonic cavity in the strong coupling regime. We focus on a red de-

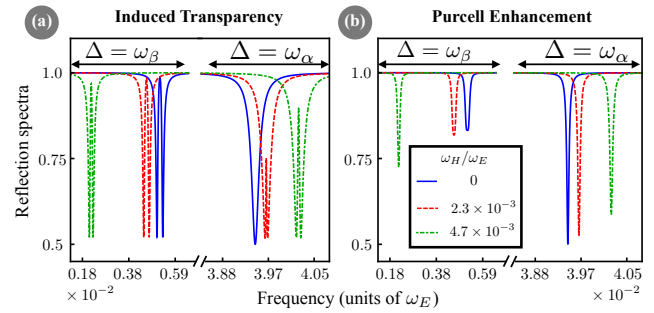


Figure 4. Reflection spectra as a function of the probe-pump detuning ω in units of ω_E for (a) the EIT regime and (b) the Purcell regime for different magnetic fields (ω_H/ω_E). Parameters: $\omega_{||}/\omega_E, \omega_{\perp}/\omega_E$ for NiO, $K = 0$, $\eta = 0.25$; (a) $\Gamma/\omega_E = 8.8 \times 10^{-6}$, $\kappa/\omega_E = 2.1 \times 10^{-4}$, $G\sqrt{n_c}/\omega_E = 1.8 \times 10^{-3}$; (b) $\Gamma/\omega_E = 2.5 \times 10^{-4}$, $\kappa/\omega_E = 6 \times 10^{-5}$, $G\sqrt{n_c}/\omega_E = 1.2 \times 10^{-3}$.

tuned control laser where the Stokes processes are far off-resonance. Following the standard procedure (see Sup. Mat. [45]) we obtain the cavity mode spectra $\delta c[\omega]$ in the frame rotating at the control light frequency

$$\delta c[\omega] = \frac{\sqrt{\eta\kappa}\delta s_{in}[\omega]}{-i(\tilde{\Delta} + \omega) + \frac{\kappa}{2} - \Sigma_\alpha(\omega) - \Sigma_\beta(\omega)}, \quad (7)$$

where $\omega = \omega_p - \omega_d$ is the pump-probe detuning, $\tilde{\Delta} = \Delta + 2G(g_\alpha \text{Re}[\langle \hat{\alpha} \rangle] + g_\beta \text{Re}[\langle \hat{\beta} \rangle])$ is the renormalized detuning due to the magnon induced cavity frequency shift with $\langle \hat{j} \rangle = iGg_j n_c / (i\omega_j + \Gamma_j/2)$ (for $j = \alpha, \beta$), and the self-energy $\Sigma_j(\omega)$ is

$$\sum_j(\omega) = \left[\frac{G^2 |g_j|^2 n_c}{-i(\omega_j + \omega) + \frac{\Gamma_j}{2}} - \frac{G^2 |g_j|^2 n_c}{i(\omega_j - \omega) + \frac{\Gamma_j}{2}} \right], \quad (8)$$

where Γ_j is the intrinsic magnon linewidth of mode j .

The transmission and reflection spectra can be obtained straightforwardly from Eq. (7) by using the input-output boundary conditions $\delta c_{out}(\omega) = \delta c_{in}(\omega) + (\kappa_c/2)^{1/2} \delta c(\omega)$. In Fig. 4 we plot the reflection spectra for different parameter regimes (for simplicity we assume $\Gamma_\alpha = \Gamma_\beta \equiv \Gamma$). In the cavity decay dominant regime ($\Gamma < g_\alpha G\sqrt{n_c} < \kappa$), an optomagnonically induced transparency peak opens in the transmission spectrum at the corresponding magnon resonance due to destructive interference between the up-converted control field and the probe field. If the magnon decay dominates ($\kappa < g_\alpha G\sqrt{n_c} < \Gamma$), a Purcell enhancement in the transmission peak at resonance is instead observed, since the magnons decay too fast for coherent beating. The results for different values of \mathbf{B}_0 demonstrate the tunability of the system.

Conclusions.— We proposed a solid state optomagnonic cavity system in which optical photons are coupled to long wavelength AFM magnons. We derived the coupling of the magnon modes to the cavity mode and showed

that (i) for easy-axis AFMs the coupling takes a simple form and it is independent of magnetic field, and (ii) in the presence of hard-axis anisotropy the coupling is tunable by a magnetic field, allowing to render a selected mode dark. We estimated the values for the coupling and showed that, although challenging, the strong coupling regime could be reached in micron sized single-domain AFMs cavities [67, 68]. In this regime, we showed that typical phenomena of cavity QED such as induced transparency and Purcell effect can occur. AFMs optical cavities could therefore provide a new platform to study

light-matter interaction, and possibly a new tool to probe AFMs due to the enhanced light-magnon coupling. The tunability with a magnetic field, in particular for tuning a magnon mode from dark to bright, shows promise for quantum protocols for quantum information storage and retrieval.

Acknowledgments.—The authors acknowledge the financial support from the Max Planck Gesellschaft through an independent Max Planck Research group. T. S. P. is grateful for discussions with A. Aiello and C. Tzscheschel. V. A. S. V. B acknowledges discussions with L. Smaldone and L. Petruzzielo.

-
- [1] X. Zhang, N. Zhu, C.-L. Zou, and H. X. Tang, Physical Review Letters **117**, 123605 (2016).
- [2] A. Osada, R. Hisatomi, A. Noguchi, Y. Tabuchi, R. Yamazaki, K. Usami, M. Sadgrove, R. Yalla, M. Nomura, and Y. Nakamura, Physical Review Letters **116**, 223601 (2016).
- [3] J. A. Haigh, A. Nunnenkamp, A. J. Ramsay, and A. J. Ferguson, Phys. Rev. Lett. **117**, 133602 (2016).
- [4] Ö. O. Soykal and M. E. Flatté, Physical Review Letters **104**, 077202 (2010).
- [5] H. Huebl, C. W. Zollitsch, J. Lotze, F. Hocke, M. Greifenstein, A. Marx, R. Gross, and S. T. B. Goennenwein, Phys. Rev. Lett. **111**, 127003 (2013).
- [6] X. Zhang, C.-L. Zou, L. Jiang, and H. X. Tang, Physical Review Letters **113**, 156401 (2014).
- [7] Y. Tabuchi, S. Ishino, T. Ishikawa, R. Yamazaki, K. Usami, and Y. Nakamura, Phys. Rev. Lett. **113**, 083603 (2014).
- [8] M. Goryachev, W. G. Farr, D. L. Creedon, Y. Fan, M. Kostylev, and M. E. Tobar, Phys. Rev. Applied **2**, 054002 (2014).
- [9] N. J. Lambert, J. A. Haigh, and A. J. Ferguson, Journal of Applied Physics **117**, 053910 (2015), <https://doi.org/10.1063/1.4907694>.
- [10] J. Bourhill, N. Kostylev, M. Goryachev, D. L. Creedon, and M. E. Tobar, Physical Review B **93**, 144420 (2016).
- [11] M. Afzelius, I. Usmani, A. Amari, B. Lauritzen, A. Walther, C. Simon, N. Sangouard, J. c. v. Minář, H. de Riedmatten, N. Gisin, and S. Kröll, Phys. Rev. Lett. **104**, 040503 (2010).
- [12] N. Sangouard, C. Simon, H. de Riedmatten, and N. Gisin, Reviews of Modern Physics **83**, 33 (2011).
- [13] N. Timoney, I. Usmani, P. Jobez, M. Afzelius, and N. Gisin, Phys. Rev. A **88**, 022324 (2013).
- [14] C.-H. Lambert, S. Mangin, B. S. D. C. S. Varaprasad, Y. K. Takahashi, M. Hehn, M. Cinchetti, G. Malinowski, K. Hono, Y. Fainman, M. Aeschlimann, and E. E. Fullerton, Science **345**, 1337 (2014).
- [15] P. Jobez, I. Usmani, N. Timoney, C. Laplane, N. Gisin, and M. Afzelius, New Journal of Physics **16**, 083005 (2014).
- [16] P. Jobez, C. Laplane, N. Timoney, N. Gisin, A. Ferrier, P. Goldner, and M. Afzelius, Phys. Rev. Lett. **114**, 230502 (2015).
- [17] M. Gündoğan, P. M. Ledingham, K. Kutluer, M. Mazzera, and H. de Riedmatten, Physical Review Letters **114**, 230501 (2015).
- [18] D. Lachance-Quirion, Y. Tabuchi, A. Gloppe, K. Usami, and Y. Nakamura, Applied Physics Express **12**, 070101 (2019).
- [19] R. Hisatomi, A. Osada, Y. Tabuchi, T. Ishikawa, A. Noguchi, R. Yamazaki, K. Usami, and Y. Nakamura, Physical Review B **93**, 174427 (2016).
- [20] J. A. Haigh, S. Langenfeld, N. J. Lambert, J. J. Baumberg, A. J. Ramsay, A. Nunnenkamp, and A. J. Ferguson, Physical Review A **92**, 063845 (2015).
- [21] A. Osada, A. Gloppe, R. Hisatomi, A. Noguchi, R. Yamazaki, M. Nomura, Y. Nakamura, and K. Usami, Physical Review Letters **120**, 133602 (2018).
- [22] A. Osada, A. Gloppe, Y. Nakamura, and K. Usami, New Journal of Physics **20**, 103018 (2018).
- [23] T. Liu, X. Zhang, H. X. Tang, and M. E. Flatté, Physical Review B **94**, 060405 (2016).
- [24] S. Viola Kusminskiy, H. X. Tang, and F. Marquardt, Physical Review A **94**, 033821 (2016).
- [25] J. Graf, H. Pfeifer, F. Marquardt, and S. Viola Kusminskiy, Physical Review B **98**, 241406 (2018).
- [26] S. Sharma, Y. M. Blanter, and G. E. W. Bauer, Physical Review Letters **121**, 087205 (2018).
- [27] V. A. S. V. Bittencourt, V. Feulner, and S. V. Kusminskiy, Physical Review A **100**, 013810 (2019).
- [28] F. Keffer and C. Kittel, Physical Review **85**, 329 (1952).
- [29] O. Gomonay, V. Baltz, A. Brataas, and Y. Tserkovnyak, Nature Physics **14** (2018), 10.1038/s41567-018-0049-4.
- [30] T. Jungwirth, J. Sinova, A. Manchon, X. Marti, J. Wunderlich, and C. Felser, Nature Physics **14** (2018), 10.1038/s41567-018-0063-6.
- [31] M. B. Jungfleisch, W. Zhang, and A. Hoffmann, Physics Letters A **382**, 865 (2018).
- [32] V. Baltz, A. Manchon, M. Tsoi, T. Moriyama, T. Ono, and Y. Tserkovnyak, Rev. Mod. Phys. **90**, 015005 (2018).
- [33] P. Wadley, B. Howells, J. elezny, C. Andrews, V. Hills, R. P. Campion, V. Novak, K. Olejnik, F. Maccherozzi, S. S. Dhesi, S. Y. Martin, T. Wagner, J. Wunderlich, F. Freimuth, Y. Mokrousov, J. Kune, J. S. Chauhan, M. J. Grzybowski, A. W. Rushforth, K. W. Edmonds, B. L. Gallagher, and T. Jungwirth, Science **351**, 587 (2016).
- [34] C. Marrows, Science **351**, 558 (2016).
- [35] M. Mergenthaler, J. Liu, J. J. Le Roy, N. Ares, A. L. Thompson, L. Bogani, F. Luis, S. J. Blundell, T. Lancaster, A. Ardavan, G. A. D. Briggs, P. J. Leek, and

- E. A. Laird, Physical Review Letters **119**, 147701 (2017).
- [36] Y. Xiao, X. H. Yan, Y. Zhang, V. L. Grigoryan, C. M. Hu, H. Guo, and K. Xia, Physical Review B **99**, 094407 (2019).
- [37] Ø. Johansen and A. Brataas, Phys. Rev. Lett. **121**, 087204 (2018).
- [38] P. Němec, M. Fiebig, T. Kampfrath, and A. V. Kimel, Nature Physics **14**, 229 (2018).
- [39] M. Aspelmeyer, T. J. Kippenberg, and F. Marquardt, Reviews of Modern Physics **86**, 1391 (2014).
- [40] R. J. Powell and W. E. Spicer, Physical Review B **2**, 2182 (1970).
- [41] M. J. Dodge, Applied Optics **23**, 1980 (1984).
- [42] I. R. Jahn, Physica Status Solidi (b) **57**, 681 (1973).
- [43] C. Kittel, *Quantum Theory of Solids*, 2nd ed. (John Wiley & Sons, New York, 1963).
- [44] T. Holstein and H. Primakoff, Physical Review **58**, 1098 (1940).
- [45] T. Parvini, V. A. S. V. Bittencourt, and S. Viola Kusminskiy, See Supplemental Material for: (I) the details on the diagonalization of the AFM Hamiltonian in terms of the Bogoliubov modes following Refs. [37, 46]; (II) Derivation of the optomagnetic Hamiltonian for antiferromagnetic systems starting with the Hamiltonian from Refs. [49, 50]; (III) symmetry considerations for deriving the properties of the optomagnetic coupling; (IV) Detailed derivation of the cavity spectra from the Heisenberg-Langevin equations [65, 69–73].
- [46] A. Kamra, U. Agrawal, and W. Belzig, Physical Review B **96**, 020411 (2017).
- [47] A. Kamra and W. Belzig, Physical Review Letters **119**, 197201 (2017).
- [48] F. L. A. Machado, P. R. T. Ribeiro, J. Holanda, R. L. Rodríguez-Suárez, A. Azevedo, and S. M. Rezende, Phys. Rev. B **95**, 104418 (2017).
- [49] M. G. Cottam and D. J. Lockwood, *Light Scattering in Magnetic Solids* (John Wiley & Sons, New York, 1986).
- [50] M. G. Cottam, Journal of Physics C: Solid State Physics **8**, 1933 (1975).
- [51] D. J. Lockwood and M. G. Cottam, Low Temperature Physics **38**, 549 (2012).
- [52] J. Ariai, P. A. Bates, M. G. Cottam, and S. R. P. Smith, Journal of Physics C: Solid State Physics **15**, 2767 (1982).
- [53] L. Bi, A. R. Taussig, H.-S. Kim, L. Wang, G. F. Dionne, D. Bono, K. Persson, G. Ceder, and C. A. Ross, Phys. Rev. B **78**, 104106 (2008).
- [54] S. Sharma, B. Z. Rameshti, Y. M. Blanter, and G. E. W. Bauer, Physical Review B **99**, 214423 (2019).
- [55] N. Brahms and D. M. Stamper-Kurn, Physical Review A **82**, 041804 (2010).
- [56] J. Kohler, N. Spethmann, S. Schreppler, and D. M. Stamper-Kurn, Physical Review Letters **118**, 063604 (2017).
- [57] M. Landini, N. Dogra, K. Kroeger, L. Hruby, T. Donner, and T. Esslinger, Physical Review Letters **120**, 223602 (2018).
- [58] R. M. Kroese, Y. Guo, V. D. Vaidya, J. Keeling, and B. L. Lev, Physical Review Letters **121**, 163601 (2018).
- [59] F. Mivehvar, H. Ritsch, and F. Piazza, Physical Review Letters **122**, 113603 (2019).
- [60] J. Barak, V. Jaccarino, and S. Rezende, Journal of Magnetism and Magnetic Materials **9**, 323 (1978).
- [61] R. C. Ohlmann and M. Tinkham, Physical Review **123**, 425 (1961).
- [62] T. Satoh, S.-J. Cho, R. Iida, T. Shimura, K. Kuroda, H. Ueda, Y. Ueda, B. A. Ivanov, F. Nori, and M. Fiebig, Physical Review Letters **105**, 077402 (2010).
- [63] T. Kampfrath, A. Sell, G. Klatt, A. Pashkin, S. Mährlein, T. Dekorsy, M. Wolf, M. Fiebig, A. Leitenstorfer, and R. Huber, Nature Photonics **5**, 31 (2011).
- [64] S. Zhou, Y. Gao, and S. Fu, The European Physical Journal B **91**, 41 (2018).
- [65] S. Weis, R. Rivière, S. Deléglise, E. Gavartin, O. Arcizet, A. Schliesser, and T. J. Kippenberg, Science **330**, 1520 (2010).
- [66] H. Xiong and Y. Wu, Applied Physics Reviews **5**, 031305 (2018).
- [67] H. Kondoh and T. Takeda, Journal of the Physical Society of Japan **19**, 2041 (1964).
- [68] J. Baruchel, M. Schlenker, K. Kurosawa, and S. Saito, Philosophical Magazine B **43**, 853 (1981).
- [69] C. W. Gardiner and P. Zoller, *Quantum Noise: A Handbook of Markovian and Non-Markovian Quantum Stochastic Methods with Applications to Quantum Optics*, 2nd ed. (Springer, Berlin, 2000).
- [70] S. M. Spillane, T. J. Kippenberg, O. J. Painter, and K. J. Vahala, Phys. Rev. Lett. **91**, 043902 (2003).
- [71] M. Cai, O. Painter, and K. J. Vahala, Phys. Rev. Lett. **85**, 74 (2000).
- [72] T. P. Purdy, P.-L. Yu, R. W. Peterson, N. S. Kampel, and C. A. Regal, Phys. Rev. X **3**, 031012 (2013).
- [73] A. H. Safavi-Naeini, T. P. M. Alegre, J. Chan, M. Eichenfield, M. Winger, Q. Lin, J. T. Hill, D. E. Chang, and O. Painter, Nature **472**, 69 (2011).

SUPPLEMENTAL MATERIAL

A. Antiferromagnetic Hamiltonian

For completeness we present here how to diagonalize the antiferromagnetic Hamiltonian

$$\hat{H}_{\text{AFM}} = \hbar \sum_{\langle i \neq j \rangle} J \hat{\mathbf{S}}^i \cdot \hat{\mathbf{S}}^j + \hbar |\gamma| \mathbf{B}_0 \cdot \sum_i \hat{\mathbf{S}}^i - \frac{\hbar K_{\parallel}}{2} \sum_i (\hat{S}_z^i)^2 + \frac{\hbar K_{\perp}}{2} \sum_i (\hat{S}_x^i)^2, \quad (9)$$

following Ref. [37]. Considering small fluctuations around equilibrium, which we set to be in the \mathbf{e}_z direction, the spin ladder operators $\hat{S}_{\pm}^i = \hat{S}_x^i \pm i \hat{S}_y^i$, and \hat{S}_z^i are given by

$$\begin{aligned} \hat{S}_+^{i \in A} &= (2S/N)^{1/2} \sum_{\mathbf{k}} e^{-i\mathbf{k} \cdot \mathbf{r}_i} \hat{a}_{\mathbf{k}}, \\ \hat{S}_+^{j \in B} &= (2S/N)^{1/2} \sum_{\mathbf{k}} e^{-i\mathbf{k} \cdot \mathbf{r}_i} \hat{b}_{\mathbf{k}}^{\dagger}, \\ S_z^{i \in A} &= S - N^{-1} \sum_{\mathbf{k}\mathbf{k}'} e^{i(\mathbf{k}-\mathbf{k}') \cdot \mathbf{r}_i} \hat{a}_{\mathbf{k}}^{\dagger} \hat{a}_{\mathbf{k}'}, \\ S_z^{j \in B} &= -S + N^{-1} \sum_{\mathbf{k}\mathbf{k}'} e^{-i(\mathbf{k}-\mathbf{k}') \cdot \mathbf{r}_i} \hat{b}_{\mathbf{k}}^{\dagger} b_{\mathbf{k}'}, \end{aligned} \quad (10)$$

where $\hat{a}_{\mathbf{k}}$ and $\hat{b}_{\mathbf{k}}$ are the collective bosonic operators associated to the sublattices A and B respectively, satisfying the commutation relations $[\hat{a}_{\mathbf{k}}, \hat{a}_{\mathbf{k}'}^\dagger] = [\hat{b}_{\mathbf{k}}, \hat{b}_{\mathbf{k}'}^\dagger] = \delta_{\mathbf{k}\mathbf{k}'}$, $[\hat{a}_{\mathbf{k}}, \hat{a}_{\mathbf{k}'}] = [\hat{a}_{\mathbf{k}}^\dagger, \hat{a}_{\mathbf{k}'}^\dagger] = [\hat{b}_{\mathbf{k}}, \hat{b}_{\mathbf{k}'}] = [\hat{b}_{\mathbf{k}}^\dagger, \hat{b}_{\mathbf{k}'}^\dagger] = 0$. S is the total spin per lattice site and N is the number of sites in each sublattice. Using Eq. 10 and keeping only terms up to two bosonic operators, \hat{H}_{AFM} is written in k -space as

$$\begin{aligned} \hat{H}_{\text{AFM}} = \hbar \sum_{\mathbf{k}} & \left[\frac{\mathcal{A}}{2} \hat{a}_{\mathbf{k}}^\dagger \hat{a}_{\mathbf{k}} + \frac{\mathcal{B}}{2} \hat{b}_{\mathbf{k}}^\dagger \hat{b}_{\mathbf{k}} + \mathcal{C}_{\mathbf{k}} \hat{a}_{\mathbf{k}} \hat{b}_{-\mathbf{k}} \right. \\ & \left. + \mathcal{D} (\hat{a}_{\mathbf{k}} \hat{a}_{-\mathbf{k}} + \hat{b}_{\mathbf{k}} \hat{b}_{-\mathbf{k}}) + h.c. \right]. \end{aligned} \quad (11)$$

The coefficients \mathcal{A} , \mathcal{B} , $\mathcal{C}_{\mathbf{k}}$ and \mathcal{D} are given in terms of the characteristic angular frequencies $\omega_E = SJZ$ (with Z the number of nearest neighbors), $\omega_{\parallel} = SK_{\parallel}$, $\omega_{\perp} = SK_{\perp}$, and $\omega_H = |\gamma| B_0$ as

$$\begin{aligned} \mathcal{A} &= (\omega_E + \omega_{\parallel} + \frac{\omega_{\perp}}{2} - \omega_H), \\ \mathcal{B} &= (\omega_E + \omega_{\parallel} + \frac{\omega_{\perp}}{2} + \omega_H), \\ \mathcal{C}_{\mathbf{k}} &= \frac{\omega_E}{Z} f(\mathbf{k}, \boldsymbol{\delta}), \quad \mathcal{D} = \frac{\omega_{\perp}}{4}, \end{aligned} \quad (12)$$

where $f(\mathbf{k}, \boldsymbol{\delta}) = \sum_j e^{-i\mathbf{k} \cdot \boldsymbol{\delta}_j}$, with the sum carried over all nearest-neighbor vectors $\boldsymbol{\delta}_j$. For long wavelength magnons $\mathcal{C}_{\mathbf{k}} \sim \omega_E$.

In order to diagonalize the Hamiltonian, we use the four-dimensional Bogoliubov transformation [37, 46]

$$\begin{bmatrix} \hat{\alpha}_{\mathbf{k}} \\ \hat{\beta}_{-\mathbf{k}} \\ \hat{\alpha}_{-\mathbf{k}}^\dagger \\ \hat{\beta}_{\mathbf{k}} \end{bmatrix} = \begin{bmatrix} u_{\alpha,a} & v_{\alpha,b} & v_{\alpha,a} & u_{\alpha,b} \\ v_{\beta,a}^* & u_{\beta,b}^* & u_{\beta,a}^* & v_{\beta,b}^* \\ v_{\alpha,a}^* & u_{\alpha,b}^* & u_{\alpha,a}^* & v_{\alpha,b}^* \\ u_{\beta,a} & v_{\beta,b} & v_{\beta,a} & u_{\beta,b} \end{bmatrix} \begin{bmatrix} \hat{a}_{\mathbf{k}} \\ \hat{b}_{-\mathbf{k}}^\dagger \\ \hat{a}_{-\mathbf{k}}^\dagger \\ \hat{b}_{\mathbf{k}} \end{bmatrix}, \quad (13)$$

where $\hat{\alpha}_{\mathbf{k}}$ and $\hat{\beta}_{\mathbf{k}}$ are the destruction operators of the bosonic magnon modes which satisfy $[\hat{\alpha}_{\mathbf{k}}, \hat{H}_{\text{AFM}}] = \hbar\omega_{\alpha k} \hat{\alpha}_{\mathbf{k}}$ and $[\hat{\beta}_{\mathbf{k}}, \hat{H}_{\text{AFM}}] = \hbar\omega_{\beta k} \hat{\beta}_{\mathbf{k}}$. These commutation relations lead to an eigenvalue problem that, together with the bosonic commutation rules for $\hat{\alpha}_{\mathbf{k}}$ and $\hat{\beta}_{\mathbf{k}}$, determine the coefficients of (13) and the eigenfrequencies $\omega_{\alpha,\beta}$ [46]. The diagonalized form of (11) is given by

$$\hat{H}_{\text{AFM}} = \hbar \sum_{\mathbf{k}} \left[\omega_{\alpha k} \hat{\alpha}_{\mathbf{k}}^\dagger \hat{\alpha}_{\mathbf{k}} + \omega_{\beta k} \hat{\beta}_{\mathbf{k}}^\dagger \hat{\beta}_{\mathbf{k}} \right]. \quad (14)$$

B. Magneto-optical Hamiltonian for Antiferromagnets

Here we present the details on the derivation of Eq. (3) in the main text starting from

$$\mathcal{H}_{\text{MO}} = \sum_i \sum_{\mu,\nu} E_{\mu}^*(\mathbf{r}_i) \varepsilon_{\mu\nu}(\mathbf{r}_i) E_{\nu}(\mathbf{r}_i), \quad (15)$$

To first order in the spins, the permittivity tensor is given by

$$\varepsilon_{\mu\nu}(\mathbf{r}_i) = \sum_{\zeta} K_{\mu\nu\zeta} S_{\zeta}^i, \quad (16)$$

with $K_{\mu\nu\zeta}$ the magneto-optical coefficients which are in general restricted by symmetry conditions. Further terms can be included to describe second order magneto-optical effects [49, 50], which we do not consider in this work.

Following Ref. [50], we assume system with a rutile crystal structure, where the two magnetic sublattices are arranged in a body-centered cubic geometry. One of the sublattices occupies the central sites, while the other occupies the corner sites. The components of the permittivity tensor are then given in terms of three imaginary constants K_1 , K_2 and K_3 [50], such that for sublattice A

$$\begin{aligned} K_{yzz}^{(A)} &= -K_{zyx}^{(A)} = K_1, \\ K_{zxy}^{(A)} &= -K_{xzy}^{(A)} = K_2, \\ K_{xyz}^{(A)} &= -K_{yxz}^{(A)} = K_3. \end{aligned} \quad (17)$$

Given the considered geometry, $K_{\mu\nu\zeta}^{(B)}$ can be obtained from $K_{\mu\nu\zeta}^{(A)}$ by $K_{\mu\nu\zeta}^{(B)} = \sum_{\mu',\nu',\zeta'} R_{\mu\mu'} R_{\nu\nu'} R_{\zeta\zeta'} K_{\mu'\nu'\zeta'}^{(A)}$ where R is the $\pi/2$ rotation matrix relating the symmetry of the sublattice A to the symmetry of the sublattice B. Therefore, for sublattice B

$$\begin{aligned} K_{yzx}^{(B)} &= -K_{zyx}^{(B)} = K_2, \\ K_{zxy}^{(B)} &= -K_{xzy}^{(B)} = K_1, \\ K_{xyz}^{(B)} &= -K_{yxz}^{(B)} = -K_3. \end{aligned} \quad (18)$$

If the sublattices are equivalent, $K_1 = K_2$.

We are interested in the optomagnetic coupling Hamiltonian, which represents the coupling of an optical field to the magnon excitations on top of the static ground state spin configuration. In correspondence with the setup of Section A, we assume that the Néel equilibrium of the AFM takes place along the e_z direction. Therefore, to first order in the magnon excitations, the coupling between light and the deviations from the magnetic equilibrium is encoded in the terms $\propto S_{x,y}$, which correspond to scattering processes involving one magnon. We thus do not consider the terms $\propto S_z$, which would correspond to higher order processes. Substituting (16), (17) and (18) in (15), the optomagnetic Hamiltonian can be written as

$$\begin{aligned} \mathcal{H}_{\text{MO}} = & \sum_{i \in A} \left[K_2 (E_z^* E_y - E_y^* E_z) S_y^i \right. \\ & \left. - K_1 (E_z^* E_x - E_x^* E_z) S_x^i \right] \\ & + \sum_{j \in B} \left[K_1 (E_z^* E_y - E_y^* E_z) S_y^j \right. \\ & \left. - K_2 (E_z^* E_x - E_x^* E_z) S_x^j \right], \end{aligned}$$

which includes contributions from each sublattice. Defining $K_{\pm} = i(K_1 \pm K_2)/4$, we obtain Eq. (2) in the main text. Quantizing it we obtain

$$\hat{\mathcal{H}}_{\text{MO}} = K_+ \sum_{\beta, \gamma} \sum_{s, s'} \sum_{i, j} \hat{c}_{\beta, s}^\dagger \hat{c}_{\gamma, s'} \left[+ P_{\beta\gamma, ss'}^{i+} \left(\hat{S}_-^i + \hat{S}_-^j \right) - P_{\beta\gamma, ss'}^{i-} \left(\hat{S}_+^i + \hat{S}_+^j \right) + K \left(P_{\beta\gamma, ss'}^{i+} \left(\hat{S}_+^i - \hat{S}_+^j \right) - P_{\beta\gamma, ss'}^{i-} \left(\hat{S}_-^i - \hat{S}_-^j \right) \right) \right],$$

where $\hat{\mathbf{E}}(\mathbf{r}, t) = \sum_{\gamma, s} \mathbf{E}_{\gamma s}(\mathbf{r}) \hat{c}_{\gamma, s}(t)$ (γ denotes the mode indices and s the polarizations), $P_{\beta\gamma, ss'}^{i\pm} = E_{\beta s, z}^*(\mathbf{r}_i) E_{\gamma s', \pm}(\mathbf{r}_i) - E_{\beta s, \pm}^*(\mathbf{r}_i) E_{\gamma s', z}(\mathbf{r}_i)$ and $K = K_-/K_+$. For modes polarized in the yz plane (as in Fig. 1 in the main text) $P_{\beta\gamma, ss'}^{i+} = -P_{\beta\gamma, ss'}^{i-} = G_{\beta\gamma, ss'}^i$, where the last equality defines the coefficients $G_{\beta\gamma, ss'}^i \equiv G_{\beta\gamma, ss'}(\mathbf{r}_i)$. Thus

$$\hat{\mathcal{H}}_{\text{MO}} = K_+ \sum_{\beta, \gamma} \sum_{i, j} G_{\beta\gamma, ss'}^i \hat{c}_{\beta, s}^\dagger \hat{c}_{\gamma, s'} \left[+ \hat{S}_-^i + \hat{S}_-^j + \hat{S}_+^i + \hat{S}_+^j + K \left(\hat{S}_+^i - \hat{S}_+^j + \hat{S}_-^i - \hat{S}_-^j \right) \right]. \quad (19)$$

In general, the total coupling coefficients will be determined by taking the continuum limit of Eq. (19), such that the sum over the lattice $\sum_{i, j}$ is replaced by integrals. The total coupling will therefore also depend on the degree of overlap of the corresponding optical and magnon modes [25].

We further specify the model by considering that only one relevant cavity mode interacts with AFM magnons with $\mathbf{k} = 0$. Moreover, we assume for simplicity that the cavity mode has a plane wave profile $\mathbf{E}(\mathbf{r}) = i \sum_{\chi=R, L} \sqrt{\frac{\hbar\omega_c}{2\varepsilon V}} e^{i\mathbf{k}_c \cdot \mathbf{r}} \mathbf{e}_\chi$, where ε is the electric permittivity of the material, V is the cavity volume, \mathbf{k}_c is the wave vector of the mode, and $\mathbf{e}_{R(L)} = (\mathbf{e}_y \mp i\mathbf{e}_z)/\sqrt{2}$ denotes right and left circularly polarized modes. For this case, using the Holstein-Primakoff approximation for the spin operators (see Eq. 10), the Hamiltonian for the right circular polarization component reads (from now on $\hat{a}_{\mathbf{k}=0} \equiv \hat{a}$ and $\hat{b}_{\mathbf{k}=0} \equiv \hat{b}$)

$$\hat{\mathcal{H}}_{\text{MO}}^R = -\hbar G \hat{c}_R^\dagger \hat{c}_R \left[\hat{a}^\dagger + \hat{b} + \hat{a} + \hat{b}^\dagger + K (\hat{a} - \hat{b}^\dagger + \hat{a}^\dagger - \hat{b}) \right], \quad (20)$$

with

$$G = \frac{\omega_c K_+}{4\varepsilon} \sqrt{2SN}. \quad (21)$$

For the left circular polarization component $\hat{\mathcal{H}}_{\text{MO}}^L = -\hat{\mathcal{H}}_{\text{MO}}^R$. Since the system is diagonal in the R/L basis,

we further consider only one circular polarization component of the optomagnetic Hamiltonian (R for definiteness) and drop the index R of (20). In order to express the optomagnetic Hamiltonian in terms of the magnon modes $\hat{a} \equiv \hat{a}_{\mathbf{k}=0}$ and $\hat{b} \equiv \hat{b}_{\mathbf{k}=0}$, we use the inverse of the transformation (13): $\hat{a} = u_{a,\alpha} \hat{a} + u_{a,\beta} \hat{b} + v_{a,\alpha} \hat{a}^\dagger + v_{a,\beta} \hat{b}^\dagger$ and $\hat{b} = u_{b,\alpha} \hat{a} + u_{b,\beta} \hat{b} + v_{b,\alpha} \hat{a}^\dagger + v_{b,\beta} \hat{b}^\dagger$. Substituting these expressions in Eq. (20) we obtain Eqs. (4) and (5) of the main text.

In the absence of hard axis anisotropy ($\omega_\perp = 0$) the non-vanishing Bogoliubov coefficients are independent of the external magnetic field and given by [46]

$$u_{a,\alpha} = u_{b,\beta} = \sqrt{\frac{\omega_E + \omega_\parallel}{\sqrt{\omega_\parallel(2\omega_E + \omega_\parallel)}}} + 1, \\ v_{a,\beta} = v_{b,\alpha} = -\sqrt{\frac{\omega_E + \omega_\parallel}{\sqrt{\omega_\parallel(2\omega_E + \omega_\parallel)}}} - 1.$$

In the limit $\omega_\parallel \ll \omega_E$ the couplings $g_{\alpha,\beta}$ take the simple form given in Eq. (6) of the main text.

In figure 5 we show the exact $g_{\alpha,\beta}$ as a function of K for $\omega_\perp = 0$ and representative values of ω_\parallel (left plot) and as a function of $\tilde{\omega}_H$ for different values of K (right plot). In the left plot, $\omega_\parallel \ll \omega_E$ and we observe a linear behavior with K , in agreement with Eq. (6) of the main text.

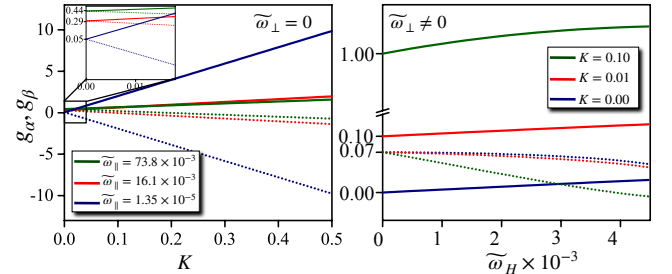


Figure 5. Couplings g_α and g_β as a function of K for $\tilde{\omega}_\perp = \omega_\perp/\omega_E = 0$ (left plot) and as a function of $\tilde{\omega}_H = \omega_H/\omega_E$ for $\tilde{\omega}_\perp = 7.6 \times 10^{-4}$. Continuous lines correspond to g_α and dotted lines to g_β . The values of $\tilde{\omega}_\parallel = \omega_\parallel/\omega_E$ and K were chosen, in increasing order, in correspondence with NiO, MnF₂ and FeF₂.

C. Symmetry Considerations

1. Zero external magnetic field case ($\omega_H = 0$ and $\omega_\perp \neq 0$)

For zero external magnetic field, the antiferromagnetic Hamiltonian is invariant under the transformation $\hat{a}_\mathbf{k} \longleftrightarrow \hat{b}_{-\mathbf{k}}$, see Eqs. 11 and 12. For $\mathbf{k} = 0$, this corresponds simply to swapping the sublattices A and B. Under this transformation $\hat{\mathcal{S}} : \hat{a} \rightarrow \hat{b}$, the Bogoliubov

modes read (remembering that for our case the Bogoliubov coefficients are all real)

$$\begin{bmatrix} \hat{\alpha}' \\ \hat{\beta}'^\dagger \\ \hat{\alpha}'^\dagger \\ \hat{\beta}' \end{bmatrix} = \begin{bmatrix} u_{\alpha,b} & v_{\alpha,a} & v_{\alpha,b} & u_{\alpha,a} \\ v_{\beta,b} & u_{\beta,a} & u_{\beta,b} & v_{\beta,a} \\ v_{\alpha,b} & u_{\alpha,a} & u_{\alpha,b} & v_{\alpha,a} \\ u_{\beta,b} & v_{\beta,a} & v_{\beta,b} & u_{\beta,a} \end{bmatrix} \begin{bmatrix} \hat{a} \\ \hat{b}^\dagger \\ \hat{a}^\dagger \\ \hat{b} \end{bmatrix} \quad (22)$$

where the prime denotes the transformed modes. Since 11 is invariant under \hat{S} , the transformed Bogoliubov modes fulfill

$$\hbar [\omega_\alpha \hat{\alpha}'^\dagger \hat{\alpha}' + \omega_\beta \hat{\beta}'^\dagger \hat{\beta}'] = \hbar [\omega_\alpha \hat{a}^\dagger \hat{a} + \omega_\beta \hat{b}^\dagger \hat{b}] . \quad (23)$$

Considering Eqs. (22) and (23), for non-degenerate modes $\omega_\alpha \neq \omega_\beta$ (this requires $\omega_\perp \neq 0$) we obtain the following conditions on the Bogoliubov coefficients: $u_{j,b} = \pm u_{j,a}$ and $v_{j,b} = \pm v_{j,a}$ (for $j = \alpha, \beta$). In our case, $\hat{\alpha}$ ($\hat{\beta}$) corresponds to the antisymmetric (symmetric) mode under the transformation:

$$\begin{aligned} u_{\alpha,b} &= -u_{\alpha,a} = -U_\alpha, \\ v_{\alpha,b} &= -v_{\alpha,a} = -V_\alpha, \\ u_{\beta,b} &= u_{\beta,a} = U_\beta, \\ v_{\beta,b} &= v_{\beta,a} = V_\beta. \end{aligned}$$

Therefore

$$\begin{bmatrix} \hat{\alpha} \\ \hat{\beta}^\dagger \\ \hat{\alpha}^\dagger \\ \hat{\beta} \end{bmatrix} = \begin{bmatrix} U_\alpha & -V_\alpha & V_\alpha & -U_\alpha \\ V_\beta & U_\beta & U_\beta & V_\beta \\ V_\alpha & -U_\alpha & U_\alpha & -V_\alpha \\ U_\beta & V_\beta & V_\beta & U_\beta \end{bmatrix} \begin{bmatrix} \hat{a} \\ \hat{b}^\dagger \\ \hat{a}^\dagger \\ \hat{b} \end{bmatrix},$$

and the inverse transformation reads

$$\begin{bmatrix} \hat{a} \\ \hat{b}^\dagger \\ \hat{a}^\dagger \\ \hat{b} \end{bmatrix} = \begin{bmatrix} U_\alpha & -V_\beta & -V_\alpha & U_\beta \\ V_\alpha & U_\beta & -U_\alpha & -V_\beta \\ -V_\alpha & U_\beta & U_\alpha & -V_\beta \\ -U_\alpha & -V_\beta & V_\alpha & U_\beta \end{bmatrix} \begin{bmatrix} \hat{\alpha} \\ \hat{\beta}^\dagger \\ \hat{\alpha}^\dagger \\ \hat{\beta} \end{bmatrix}, \quad (24)$$

where we have used that $2(|U_j|^2 - |V_j|^2) = 1$. From $g_j = (u_j^+ + v_j^+) + K(u_j^- + v_j^-)$ we obtain

$$\begin{aligned} g_\alpha &= 2K(U_\alpha - V_\alpha), \\ g_\beta &= 2(U_\beta - V_\beta) \end{aligned}$$

and hence for $K = 0$ the α -mode is decoupled from the light, while the β -mode coupling is independent of K .

2. Easy axis AFM case ($\omega_\perp = 0$)

In the absence of hard axis anisotropy, the Hamiltonian 9 is invariant under rotations around the e_z axis and 11 reads (for $\mathbf{k} = 0$, and $\hbar = 1$)

$$\hat{H}_{\text{AFM}} = \mathcal{A}\hat{a}^\dagger \hat{a} + \mathcal{B}\hat{b}^\dagger \hat{b} + \mathcal{C}(\hat{a}\hat{b} + \hat{a}^\dagger \hat{b}^\dagger), \quad (25)$$

A rotation by θ around the e_z axis is given by $\hat{\mathcal{R}} : \hat{S}_+ \rightarrow e^{i\theta}\hat{S}_+$, thus at the level of the bosonic operators $\hat{a} \rightarrow e^{i\theta}\hat{a}$ and $\hat{b} \rightarrow e^{-i\theta}\hat{b}$. The Bogoliubov modes transform as

$$\begin{aligned} \hat{\alpha} &= e^{i\theta} (u_{\alpha,a}\hat{a} + v_{\alpha,b}\hat{b}^\dagger) + e^{-i\theta} (u_{\alpha,b}\hat{b} + v_{\alpha,a}\hat{a}^\dagger), \\ \hat{\beta} &= e^{i\theta} (u_{\beta,a}\hat{a} + v_{\beta,b}\hat{b}^\dagger) + e^{-i\theta} (u_{\beta,b}\hat{b} + v_{\beta,a}\hat{a}^\dagger). \end{aligned}$$

We thus conclude that, in order for $\hat{H}_{\text{AFM}} = \omega_\alpha \hat{\alpha}^\dagger \hat{\alpha} + \omega_\beta \hat{\beta}^\dagger \hat{\beta}$ to be invariant we have (for $j = \alpha, \beta$) $u_{j,a} = v_{j,b} = 0$ or $u_{j,b} = v_{j,a} = 0$. In our case, $\hat{\mathcal{R}} : \hat{a} \rightarrow e^{i\theta}\hat{a}$ and $\hat{\beta} \rightarrow e^{-i\theta}\hat{\beta}$, thus fixing $u_{\alpha,a} = U_\alpha$, $v_{\alpha,b} = V_\alpha$, $u_{\beta,b} = U_\beta$, $v_{\beta,a} = V_\beta$ and $u_{\alpha,b} = u_{\beta,a} = v_{\alpha,a} = v_{\beta,b} = 0$. We can then write \hat{H}_{AFM} in terms of the Bogoliubov coefficients (besides a constant term) as

$$\begin{aligned} \hat{H}_{\text{AFM}} &= (\omega_\alpha U_\alpha^2 + \omega_\beta V_\beta^2)\hat{a}^\dagger \hat{a} + (\omega_\beta U_\beta^2 + \omega_\alpha V_\alpha^2)\hat{b}^\dagger \hat{b} \\ &\quad + (\omega_\alpha U_\alpha V_\alpha + \omega_\beta U_\beta V_\beta)(\hat{a}\hat{b} + \hat{a}^\dagger \hat{b}^\dagger). \end{aligned} \quad (26)$$

Comparing the above expression with (25) we have

$$\begin{aligned} \omega_\alpha U_\alpha^2 + \omega_\beta V_\beta^2 &= \mathcal{A}, \\ \omega_\beta U_\beta^2 + \omega_\alpha V_\alpha^2 &= \mathcal{B}, \end{aligned}$$

and thus, using $U_j^2 - V_j^2 = 1$

$$\omega_\alpha - \omega_\beta = \mathcal{A} - \mathcal{B} = -2\omega_H. \quad (27)$$

To obtain further information on the form of the Bogoliubov coefficients we use the eigenvalue equations to obtain

$$\begin{cases} (\mathcal{A} - \omega_\alpha)U_\alpha - \mathcal{C}V_\alpha &= 0, \\ \mathcal{C}U_\alpha - (\mathcal{B} + \omega_\alpha)V_\alpha &= 0, \end{cases} \quad (28)$$

$$\begin{cases} -(\mathcal{A} + \omega_\beta)V_\beta + \mathcal{C}U_\beta &= 0, \\ -\mathcal{C}V_\beta + (\mathcal{B} - \omega_\beta)U_\beta &= 0. \end{cases} \quad (29)$$

Using (27) we can rearrange Eq. (29) into

$$\begin{cases} (\mathcal{A} - \omega_\alpha)U_\beta - \mathcal{C}V_\beta &= 0, \\ \mathcal{C}U_\beta - (\mathcal{B} + \omega_\alpha)V_\beta &= 0. \end{cases}$$

Comparing with (28) we conclude that $U_\beta = U_\alpha = U$ and $V_\beta = V_\alpha = V$. Finally we notice that since $\omega_\alpha = -\omega_H + \frac{1}{2}\sqrt{(\mathcal{A} + \mathcal{B})^2 - 4\mathcal{C}^2}$, $\mathcal{A} = -\omega_H + \omega_E + \omega_\parallel$ and $\mathcal{B} = \omega_H + \omega_E + \omega_\parallel$, then $\mathcal{A} - \omega_\alpha$ and $\mathcal{B} + \omega_\alpha$ are independent of ω_H , and hence the Bogoliubov coefficients U and V are independent of ω_H . Therefore the couplings

$$\begin{aligned} g_\alpha &= U - V + K(U + V), \\ g_\beta &= U - V - K(U + V) \end{aligned} \quad (30)$$

are independent of the magnetic field for $\omega_\perp = 0$ and at $K = 0$ they have equal strength $g_\alpha = g_\beta$. In this derivation the important fact was $u_{\alpha,b} = u_{\beta,a} = v_{\alpha,a} = v_{\beta,b} = 0$, which is consequence of the invariance under rotations around the e_z axis.

3. Degenerate case $\omega_H = \omega_{\perp} = 0$

For $\omega_H = \omega_{\perp} = 0$, under $\hat{\mathcal{S}} : \hat{a} \rightarrow \hat{b}$ we have $\hat{\mathcal{S}}\hat{a}\hat{S}^{-1} = \hat{b}$, and the diagonalized Hamiltonian Eq. (23) is invariant since $\omega_{\alpha} = \omega_{\beta}$. This falls into the previous case and the couplings $g_{\alpha,\beta}$ are given by Eqs. (30).

Note that the Bogoliubov coefficients present a discontinuity at $\omega_{\perp} = 0$ and therefore also the $g_{\alpha,\beta}$. In particular, $g_{\alpha}(\omega_H = 0, K = 0) = 0$ for $\omega_{\perp} \neq 0$ as we showed in Subsection A, but it is finite for $\omega_{\perp} = 0$, see Subsection B and Eq. (6) in the main text.

D. Equations of motion for the control-probe pump scheme

In this section we derive the cavity spectra of the antiferromagnetic optomagnonic system by solving the linearized quantum Langevin equations. The total Hamiltonian of the driven optomagnonic cavity, under the simplifications of the previous sections, reads

$$\begin{aligned} \hat{H} = & \hbar\omega_c\hat{c}^{\dagger}\hat{c} + \hbar\omega_{\alpha}\hat{\alpha}^{\dagger}\hat{\alpha} + \hbar\omega_{\beta}\hat{\beta}^{\dagger}\hat{\beta} \\ & - \hbar G\hat{c}^{\dagger}\hat{c}(g_{\alpha}\hat{\alpha}^{\dagger} + g_{\beta}\hat{\beta}^{\dagger} + \text{h.c.}) + \hat{H}_{\text{drive}}. \end{aligned}$$

The intracavity field is driven by input lasers which can be described by the Hamiltonian $\hat{H}_{\text{drive}} = i\hbar\sqrt{\eta\kappa}(s_{\text{in}}(t)\hat{a}^{\dagger} - s_{\text{in}}^{*}(t)\hat{a})$, where $s_{\text{in}}(t) = (s_d e^{-i\omega_d t} + s_p e^{-i\omega_p t})$ is the amplitude of the drive normalized to the input photon flux and ω_d (ω_p) is the control (probe) laser frequency, with $s_{d,p} = \sqrt{\frac{2\mathcal{P}_{d,p}}{\hbar\omega_{d,p}}}$ given in terms of the drive powers $\mathcal{P}_{d,p}$. The total cavity loss rate is denoted by $\kappa = \kappa_0 + \kappa_{\text{ex}}$, where κ_0 denotes the intrinsic loss rate and κ_{ex} the external loss rate. The dimensionless parameter $\eta \equiv \kappa_{\text{ex}}/(\kappa_0 + \kappa_{\text{ex}})$, can be continuously adjusted in experiments [70, 71]. In this control-probe scheme, the control laser has a stronger intensity than the probe laser $s_d \gg s_p$ [39, 65, 73]. In a frame rotating with the control laser frequency, the total Hamiltonian reads

$$\begin{aligned} \hat{H} = & -\hbar\Delta\hat{c}^{\dagger}\hat{c} + \hbar\omega_{\alpha}\hat{\alpha}^{\dagger}\hat{\alpha} + \hbar\omega_{\beta}\hat{\beta}^{\dagger}\hat{\beta} \\ & - \hbar G\hat{c}^{\dagger}\hat{c}(g_{\alpha}\hat{\alpha}^{\dagger} + g_{\beta}\hat{\beta}^{\dagger} + \text{h.c.}) \\ & + i\hbar\sqrt{\eta\kappa}\left[\left(s_d + s_p e^{-i(\omega_p - \omega_d)t}\right)\hat{a}^{\dagger} - \text{h.c.}\right], \end{aligned}$$

where $\Delta = \omega_d - \omega_c$ is the detuning between the cavity and the control laser frequency. The Langevin equations of motion for the operators $\hat{\alpha}$, $\hat{\beta}$ and \hat{c} are thus

$$\begin{aligned} \dot{\hat{\alpha}} = & -\left(i\omega_{\alpha} + \frac{\Gamma_{\alpha}}{2}\right)\hat{\alpha} + iGg_{\alpha}\hat{c}^{\dagger}\hat{c} + \sqrt{\Gamma_{\alpha}}\hat{\alpha}_{\text{noise}}(t), \\ \dot{\hat{\beta}} = & -\left(i\omega_{\beta} + \frac{\Gamma_{\beta}}{2}\right)\hat{\beta} + iGg_{\beta}\hat{c}^{\dagger}\hat{c} + \sqrt{\Gamma_{\beta}}\hat{\beta}_{\text{noise}}(t), \\ \dot{\hat{c}} = & \left(i\Delta - \frac{\kappa}{2}\right)\hat{c} + iG\hat{c}\left[g_{\alpha}(\hat{\alpha} + \hat{\alpha}^{\dagger}) + g_{\beta}(\hat{\beta} + \hat{\beta}^{\dagger})\right] \\ & + \sqrt{\eta\kappa}s_d + \sqrt{(1-\eta)\kappa}\hat{c}_{\text{noise}}(t), \end{aligned}$$

with $\Gamma_{\alpha,\beta}$ is the intrinsic magnon damping rates which we assume to be equal $\Gamma_{\alpha} = \Gamma_{\beta} = \Gamma$. We have disregarded, for now, the effects of the weak probe pump since $s_d \gg s_p$. Here and in what follows, the noise operators describe random fluctuations of the system and have vanishing expectation values [69]. We consider the equations for the expectations values $\langle\hat{\alpha}\rangle$, $\langle\hat{\beta}\rangle$ and $\langle\hat{c}\rangle$, disregarding quantum fluctuations, such that for example $\langle\hat{c}^{\dagger}\hat{c}\rangle = |\langle\hat{c}\rangle|^2$. The steady state is obtained by setting $\langle\dot{\hat{c}}\rangle \equiv \dot{\bar{c}} = 0$, $\langle\dot{\hat{\alpha}}\rangle = 0$ and $\langle\dot{\hat{\beta}}\rangle = 0$, such that

$$\begin{aligned} \langle\hat{\alpha}\rangle &= \frac{iGg_{\alpha}|\bar{c}|^2}{i\omega_{\alpha} + \frac{\Gamma}{2}}, \\ \langle\hat{\beta}\rangle &= \frac{iGg_{\beta}|\bar{c}|^2}{i\omega_{\beta} + \frac{\Gamma}{2}}, \\ \bar{c} &= \frac{-\sqrt{\eta\kappa}s_d}{(i\Delta - \frac{\kappa}{2}) + 2iG\left(g_{\alpha}\text{Re}[\langle\hat{\alpha}\rangle] + g_{\beta}\text{Re}[\langle\hat{\beta}\rangle]\right)}. \end{aligned}$$

We linearize the dynamics of the system by considering the fluctuations over the steady state values $\hat{\alpha}(t) = \langle\hat{\alpha}\rangle + \delta\hat{\alpha}(t)$, $\hat{\beta}(t) = \langle\hat{\beta}\rangle + \delta\hat{\beta}(t)$ and $\hat{c}(t) = \bar{c} + \delta\hat{c}(t)$. Correspondingly for the input field $s_{\text{in}}(t) = \bar{s} + \delta s_{\text{in}}(t)$, where we identify $\bar{s} = s_d$ as the amplitude of the control field due to $s_d \gg s_p$. The linearized Langevin equations for the fields' fluctuations read

$$\begin{aligned} \delta\dot{\hat{\alpha}} = & -\left(i\omega_{\alpha} + \frac{\Gamma}{2}\right)\delta\hat{\alpha} + iGg_{\alpha}(\bar{c}\delta\hat{c}^{\dagger} + \bar{c}^*\delta\hat{c}) \\ & + \sqrt{\Gamma}\delta\hat{\alpha}_{\text{noise}}(t), \\ \delta\dot{\hat{\beta}} = & -\left(i\omega_{\beta} + \frac{\Gamma}{2}\right)\delta\hat{\beta} + iGg_{\beta}(\bar{c}\delta\hat{c}^{\dagger} + \bar{c}^*\delta\hat{c}) \\ & + \sqrt{\Gamma}\delta\hat{\beta}_{\text{noise}}(t), \\ \delta\dot{\hat{c}} = & \left(i\tilde{\Delta} - \frac{\kappa}{2}\right)\delta\hat{c} + iG\bar{c}\left(g_{\alpha}\delta\hat{\alpha}^{\dagger} + g_{\beta}\delta\hat{\beta}^{\dagger} + \text{h.c.}\right) \\ & + \sqrt{\eta\kappa}\delta s_{\text{in}}(t) + \sqrt{\kappa}\delta\hat{c}_{\text{noise}}(t). \end{aligned}$$

In these equations $\tilde{\Delta} = \Delta + 2G(g_{\alpha}\text{Re}[\langle\hat{\alpha}\rangle] + g_{\beta}\text{Re}[\langle\hat{\beta}\rangle])$ takes into account the cavity frequency shift due to the coupling to the magnon modes.

Finally, we obtain the mode spectra via the Langevin equations for the average values of the fluctuations in frequency space. Defining the Fourier transform as $\delta X[\omega] = \int_{-\infty}^{\infty} dt e^{-i\omega t}\langle\delta\hat{X}(t)\rangle$ for $X = \delta\alpha^{(\dagger)}, \delta\beta^{(\dagger)}, \delta c^{(\dagger)}$ [72] the Langevin equations read

$$\begin{aligned} \left[i(\omega_{\alpha} - \omega) + \frac{\Gamma}{2}\right]\delta\alpha[\omega] &= iGg_{\alpha}(\bar{c}\delta c^*[-\omega] + \bar{c}^*\delta c[\omega]), \\ \left[i(\omega_{\beta} - \omega) + \frac{\Gamma}{2}\right]\delta\beta[\omega] &= iGg_{\beta}(\bar{c}\delta c^*[-\omega] + \bar{c}^*\delta c[\omega]), \\ \left[-i(\tilde{\Delta} + \omega) + \frac{\kappa}{2}\right]\delta c[\omega] &= iG\bar{c}\left(g_{\alpha}(\delta\alpha^*[-\omega] + \delta\alpha[\omega])\right. \\ &\quad \left.+ g_{\beta}(\delta\beta^*[-\omega] + \delta\beta[\omega])\right) \\ &+ \sqrt{\eta\kappa}\delta s_{\text{in}}[\omega]. \end{aligned}$$

The cavity spectrum is thus

$$\delta c[\omega] = \frac{(1 + F(\omega))\sqrt{\eta\kappa}\delta s_{\text{in}}[\omega]}{-i(\tilde{\Delta} + \omega) + \frac{\kappa}{2} - 2i\tilde{\Delta}F(\omega)},$$

where

$$F(\omega) = \frac{\Sigma(\omega)}{i(\tilde{\Delta} - \omega) + \frac{\kappa}{2}},$$

with $\Sigma(\omega)$ the self-energy term given by

$$\begin{aligned} \Sigma(\omega) &= G^2|\bar{c}|^2 \\ &\left[-\frac{g_\alpha^2}{i(\omega_\alpha - \omega) + \frac{\Gamma}{2}} + \frac{g_\alpha^2}{-i(\omega_\alpha + \omega) + \frac{\Gamma}{2}} + \right. \\ &\left. -\frac{g_\beta^2}{i(\omega_\beta - \omega) + \frac{\Gamma}{2}} + \frac{g_\beta^2}{-i(\omega_\beta + \omega) + \frac{\Gamma}{2}} \right]. \end{aligned}$$

Since we are working in a rotating frame with the control laser, the frequency ω is the sideband shift of the probe ω_p from the control light frequency, $\omega = \omega_p - \omega_d$. In the following and in the main text we restrict our results to the resolved sideband regime case, $\omega_{\alpha,\beta} \gg \kappa$. For a red detuned control drive ($\tilde{\Delta} < 0$), Stoke's processes are far off-resonance and the relevant resonance is $\tilde{\Delta} \approx -\omega \approx -\omega_{\alpha,\beta}$. In this case we can approximate $F(\omega) \sim \Sigma(\omega)/2i\tilde{\Delta}$ and, if $\tilde{\Delta} \gg \Sigma(\omega)$, then the cavity spectrum is given by

$$\delta c_{\tilde{\Delta} < 0}[\omega] = \frac{\sqrt{\eta\kappa}\delta s_{\text{in}}[\omega]}{-i(\tilde{\Delta} + \omega) + \frac{\kappa}{2} - \Sigma_{\text{AS}}(\omega)}, \quad (31)$$

where $\Sigma_{\text{AS}} = -\frac{g_\alpha^2}{i(\omega_\alpha - \omega) + \Gamma/2} - \frac{g_\beta^2}{i(\omega_\beta - \omega) + \Gamma/2}$. The input-output boundary conditions $\delta s_{\text{out}}[\omega] = \delta s_{\text{in}}[\omega] - \sqrt{\eta\kappa}\delta c[\omega]$ thus yield to the transmission amplitude $t = \delta s_{\text{out}}[\omega]/\delta s_{\text{in}}[\omega]$, and to the reflection coefficient $|r|^2 = 1 - |t|^2$.

Analogously, we can obtain the magnon linewidth $\tilde{\Gamma}_j = \Gamma + 2\text{Re}[\tilde{\Sigma}_j]$ and frequency shift $\delta\omega_j = \text{Im}[\tilde{\Sigma}_j]$ ($j = \alpha, \beta$) in terms of (for $k \neq j$, and omitting the dependences on ω)

$$\begin{aligned} \tilde{\Sigma}_j[\omega] &= -\xi_j(1 + X_j) + \xi_{jk}X_k \\ &- \frac{\xi_jX_j + \xi_{jk}(X_k + 1)}{\chi_j^{-1} - \xi_j(1 + X_j) + \xi_{jk}X_k} (\xi_kX_k + \xi_{jk}(1 + X_j)), \end{aligned} \quad (32)$$

with

$$\begin{aligned} \xi_j[\omega] &= G^2|\bar{c}|^2g_j^2 \left[\frac{1}{i(\tilde{\Delta} - \omega) + \frac{\kappa}{2}} - \frac{1}{-i(\tilde{\Delta} + \omega) + \frac{\kappa}{2}} \right], \\ \xi_{jk}[\omega] &= \sqrt{\xi_j[\omega]\xi_k[\omega]}, \\ \chi_j[\omega] &= \left[i(\omega_j - \omega) + \frac{\Gamma}{2} \right]^{-1}, \\ X_j[\omega] &= - \left[\chi_j^*[-\omega] + \xi_j[\omega] - \frac{\xi_{jk}[\omega]}{\chi_k^*[-\omega] + \xi_k[\omega]} \right]^{-1} \\ &\times \xi_j[\omega] \left[\frac{\xi_k}{\chi_k^*[-\omega] + \xi_k} - 1 \right]. \end{aligned}$$

Under the same assumptions leading to (31), (32) is given by

$$\tilde{\Sigma}_j[\omega] \approx \frac{G^2|\bar{c}|^2g_j^2}{-i(\tilde{\Delta} + \omega) + \frac{\kappa}{2}},$$

and the magnon linewidth and frequency shift are given by

$$\begin{aligned} \delta\omega_j[\omega] &\approx \frac{G^2|\bar{c}|^2g_j^2(\tilde{\Delta} + \omega)}{(\tilde{\Delta} + \omega)^2 + \frac{\kappa^2}{4}}, \\ \tilde{\Gamma}_j &\approx \Gamma + \frac{G^2|\bar{c}|^2g_j^2\kappa}{(\tilde{\Delta} + \omega)^2 + \frac{\kappa^2}{4}}. \end{aligned}$$